

MICROTURBULENCE, SYSTEMATIC MOTIONS, AND LINE FORMATION IN MOLECULAR CLOUDS*

RICHARD E. WHITE

Goddard Institute for Space Studies;† and Five College Astronomy Department, Smith College, Northampton, Massachusetts

Received 1975 October 14; revised 1976 July 23

ABSTRACT

Microturbulence and systematic motions are viewed as simplifying assumptions made to facilitate treatment of line formation in molecular clouds, and line intensities calculated in the two approximations are compared to estimate how uncertainties about the actual line-broadening mechanism affect the interpretation of molecular emission lines. For lines formed by two-level molecules in an isothermal homogeneous cloud, the alternative assumptions lead to peak and integrated line intensities which agree within the differences (up to a factor of 3) associated with the ignorance of cloud geometry. New multilevel calculations for CO in the same cloud model bear out the generality of this result. It follows that, within the geometrical uncertainties, the Sobolev approximation may be used confidently in the numerous applications for which this simple cloud model suffices.

Subject headings: interstellar: molecules — line formation — line profiles — nebulae: general — radiative transfer

I. INTRODUCTION

The mechanisms which broaden the spectral lines emitted by molecular clouds are poorly understood. The lines are almost invariably too wide to be explained by thermal motions, and they frequently imply supersonic velocities. The line widths have commonly been attributed to turbulence, but difficulties with line profile interpretation and energetic difficulties associated with supersonic turbulence have led to the supposition that the line widths reflect systematic motions within the clouds, presumably large-scale collapse (Goldreich and Kwan 1974; Scoville and Solomon 1974; Liszt *et al.* 1974). However, other evidence seems to weigh against the notion that collapse generally dominates the line widths (Zuckerman and Evans 1974; Morris *et al.* 1974), and has led to alternative suggestions that the lines reflect the existence of unresolved fragmentation (Zuckerman and Evans 1974) or the presence of hydromagnetic waves (Arons and Max 1975).

The form of the velocity field has an important bearing on the interpretation of the molecular line observations. In general, the cloud densities are too low for collisions to thermalize the populations of the molecular energy levels; thus the molecular excitation, and hence the observed line intensities, depend on the degree to which radiative trapping thermalizes the line radiation field. If systematic motions introduce Doppler shifts far in excess of the local Doppler widths, molecules can interact radiatively only within

a small volume; trapping is *local* and can be treated in a straightforward way (Goldreich and Kwan 1974; Scoville and Solomon 1974; White 1973) which is referred to hereafter as the "Sobolev approximation" (Sobolev 1960). More generally, scattered radiation makes a significant *nonlocal* contribution to the molecular excitation. Then numerical treatment is much more complex, even in the simplest case, where it is assumed that the cloud has no large-scale motions and that the lines have a Doppler profile due to a combination of thermal motions and small-scale random motions, "microturbulence" (White 1971, 1973; Clark, Buhl, and Snyder 1974; Lucas 1974; Leung 1975; Leung and Liszt 1976). Hereafter, this case is referred to as the "microturbulent approximation."

Both microturbulence and simple collapse are idealized motions, and neither may accurately represent the velocities in molecular clouds. Therefore this paper investigates quantitatively how the choice of velocity model may influence the interpretation of molecular line observations. In § II it is argued that the two velocity models can be viewed as approximate limiting cases for the treatment of molecular line formation. Consequently, a comparison of the intensities predicted in the two approximations for otherwise identical cloud models yields a fair estimate of the uncertainties associated with the velocity field. For isothermal homogeneous cloud models (§ III), new microturbulent calculations and Sobolev calculations, both for a two-level molecule and for carbon monoxide, yield line intensities which agree within the approximately threefold uncertainty associated with cloud geometry. The implications and limitations of the calculations are discussed in § IV.

* This is contribution No. 216 of the Five College Observatories.

† National Academy of Sciences-National Research Council Resident Research Associate.

II. MICROTURBULENCE AND SYSTEMATIC MOTIONS AS LIMITING APPROXIMATIONS

The idea that large-scale motions develop in molecular clouds as a result of gravitational instability provides a plausible rationale for use of the Sobolev approximation in studies of molecular line formation (Goldreich and Kwan 1974). The idea that *micro*-turbulence occurs in molecular clouds is implausible, because it requires that the motions have a characteristic length scale which is short compared with the photon mean free path. Rotational lines of abundant molecules in dense interstellar clouds, where the thermal line widths are $\sim 0.1 \text{ km s}^{-1}$, have photon mean free paths which are but a small fraction of the cloud size. It is uncertain, and seems unlikely, that turbulence, density inhomogeneities, or hydromagnetic waves will be restricted to the small scale required. So it becomes necessary to consider the effects of *macro*turbulence on the molecular source functions and line profiles.¹ In the course of this discussion, we develop the rationale that the assumption of microturbulence is useful as a limiting approximation, and that the Sobolev approximation represents the alternative limiting case, whether or not collapse dominates the motions in molecular clouds.

Line profiles are exceedingly sensitive to the velocity fields present in the line-forming regions. The microturbulent approximation yields the prediction that optically thick lines will be symmetrical and self-reversed under most circumstances, with the result that isotopic variants of an abundant molecule, particularly ^{12}CO and ^{13}CO , should have very different line profiles. Although some evidence for self-reversed ^{12}CO lines has appeared (Kutner and Tucker 1975), observers have used the much more common absence of this effect to argue against the notion of turbulent line broadening (Liszt *et al.* 1974). However, systematic velocities only twice the thermal velocity seriously and systematically distort the self-reversed line profiles, while producing only modest differences from the microturbulent source functions (Kunasz and Hummer 1974b). Macroturbulence will almost certainly produce comparable, but irregular, changes in line shape. This circumstance obviates the line profile argument against turbulent line broadening, but it will often limit application of the microturbulent approximation to cases where attention is restricted to the peak and integrated intensities of the lines (as in § III), or where a more realistic velocity field is adopted in the line profile calculations.

Within these limitations, the relevance of the microturbulent approximation hinges on its utility in the more difficult problem of determining the molecular source functions. For the homogeneous velocity field assumed in the microturbulent approximation, the source functions are generally coupled throughout the cloud by scattered radiation; for the

¹ For the purpose of this discussion, macroturbulence refers to any motion which has a scale comparable to or exceeding the photon mean free path. This includes hydrodynamic turbulence, macroscopic motion of cloud fragments, and hydromagnetic waves.

large-amplitude systematic motions assumed in the Sobolev approximation, the local source functions are independent of one another. The crucial difference here is not between microturbulent and systematic motions, but between nonlocal and local radiative excitation. Like systematic motions, macroturbulence probably tends to decouple neighboring parts of the cloud; but it may or may not isolate local regions from the rest of the cloud. So, we reason that the source functions of optically thick lines in the presence of macroturbulence will approach those found in the microturbulent (Sobolev) approximation to the degree that radiative interaction between distant parts of the cloud is strong (weak). And in the intermediate cases, we expect a smooth variation away from the microturbulent (Sobolev) source functions, like that found by Kunasz and Hummer (1974b) for small-amplitude systematic motions.

We conclude that the microturbulent and Sobolev approximations may usefully be viewed as limiting cases for the determination of molecular line source functions, and that comparison of the peak and integrated line intensities given by the two approximations for otherwise identical cloud models will indicate the effects which uncertainties in the velocity field have on the interpretation of molecular line data. Section III presents such a comparison for a very simple but commonly used cloud model.

III. THE ISOTHERMAL HOMOGENEOUS CLOUD

The restriction of line-formation calculations to simple geometrical configurations introduces a fundamental limitation to the accuracy of theoretical studies of molecular cloud spectra. Hence we view the geometrical variations in line strength as a standard for assessing the influence of the velocity field, and present calculations for the microturbulent and Sobolev approximations in both plane-parallel and spherical geometry. Part (a) of this section outlines the numerical formulation of the microturbulent and Sobolev calculations. Part (b) presents results obtained for a two-level molecule. In this case the effects of temperature, density, and optical depth can be accounted for in a compact way, which clearly isolates and demonstrates the effects of the velocity field and the cloud geometry. Part (c) extends the results to carbon monoxide, showing that the influence of velocity field and geometry are accurately illustrated by the two-level calculations.

a) Numerical Formulation

i) Microturbulent Approximation

The radiative transfer problem posed in the microturbulent approximation is global and nonlinear, because scattered photons allow interaction between distant parts of the cloud, and because multipole collisions allow interaction between different lines. The problem demands a simultaneous self-consistent solution for the radiation field in the spectral lines and for the occupation numbers of the molecular energy levels throughout the cloud.

We have solved this problem in plane-parallel geometry using a variation of the linearization technique described by Auer (1971). With the adoption of variable Eddington factors to relate the moments of the specific intensity, the equation of transfer at each discrete frequency takes the form of a second-order differential equation for the mean intensity, with the appropriate boundary conditions. A difference scheme in depth transforms each differential equation and its boundary conditions into a system of algebraic equations. The physical conditions are specified, so these equations can be solved subject only to the constraint imposed by the statistical equilibrium equations at each depth point. The difference equations are linearized to yield expressions involving corrections to the adopted trial values of the mean intensities and corrections to the adopted energy level populations, while the latter are eliminated by means of the linearized statistical equilibrium equations (Auer 1973). As suggested by Auer's (1971) discussion, *complete* linearization of the problem was unnecessary for the work reported here. The simple radiative selection rules ($\Delta J = \pm 1$) which govern rotational transitions of linear molecules allow successive solutions of the linearized equations for the radiation in each line rather than simultaneous solution of all the equations. This line-by-line approach makes it economical to retain the Feautrier (1964) method for solving the transfer equations, rather than adopting the modified Feautrier technique (Rybicki 1971).

The solution proceeds iteratively. A trial set of occupation numbers, described below, determine the line opacities and source functions needed to calculate the trial intensities by formal solution of the transfer equations. The new intensities yield the radiative transition rates; then solution of the statistical equilibrium equations provides improved estimates of the occupation numbers.² At each iteration the current estimates of the mean intensities and occupation numbers determine the coefficients of the linearized equations, which are solved line by line, first $J = 1 \rightarrow 0$, then $J = 2 \rightarrow 1$, and so on. The intensity corrections for each line are used to improve the radiative transition rates, and the occupation numbers are correspondingly revised before the solution for the next line is begun. After all the lines have been treated, the fractional mean intensity corrections are calculated; another iteration begins if any of the fractional corrections exceeds a prescribed limit, which was 0.1% in the work reported here. The line-by-line solutions typically require five to 10 iterations, not more than 3 times the number required if all the linearized equations are solved at once; while the computation time per iteration may be smaller by one to two orders of magnitude, depending on the number of lines treated. The computation time varies approximately linearly with the number of lines considered, the number of depth points used, and

² Repetition of this sequence (Λ -iteration) represents the most obvious approach to the problem, but it may fail under many important circumstances (Mihalas 1970, p. 214).

the number of iterations required. To cite a single case, a solution involving 10 lines, 20 depth points, and seven iterations took 27 seconds on an IBM 360/95.

The proper choice of trial solutions is crucial to the stability of the linearization scheme. To ensure adequate initial estimates, a set of calculations for a given density and temperature begins at low projected density of molecules (N), so that the optically thin statistical equilibrium solutions apply. The computations proceed to successively larger values of N at intervals of 0.5 dex. In each case after the second one, the molecular occupation numbers (n_j) are extrapolated from the two preceding cases:

$$\ln (n_j)_{i+1} = \ln (n_j)_i + f[\ln (n_j)_i - \ln (n_j)_{i-1}].$$

Values of $f \approx 0.4$ give the most satisfactory convergence. We have encountered no convergence problems using this approach, even in cases where the $J = 1 \rightarrow 0$ line of CO has inverted populations (Goldsmith 1972).

Simplifying assumptions and parameter choices made in the calculations include the following. The assumption that photons scatter isotropically with complete redistribution in frequency renders the source functions independent of frequency across each line. The Eddington approximation fixes the Eddington factors throughout the calculations. Only half the line is treated explicitly, because of the symmetry of the line profile; the discrete frequencies are spaced uniformly from the line center to a frequency 4.5 Doppler widths away, at intervals of 0.5 Doppler units for the source function calculations, and at intervals of 0.25 Doppler units for the emergent intensity solutions. Except at the cloud surface, the discrete depth points are spaced at intervals of 0.25 dex in projected density. With these parameters, our two-level Eddington approximate calculations agree with those of Avrett and Hummer (1965) within a few percent, while the Eddington approximation itself provides about 10% accuracy (Avrett and Hummer 1965). The formal accuracy associated with the assumption of complete redistribution is probably poorer than this (Hummer 1969); but, given the uncertainty in the line-broadening mechanism, a more precise treatment is unwarranted.

The multilevel calculations treat cases that have a wide range of excitation conditions in a single run. Consequently, the total number of transitions included and the number treated self-consistently are varied from one case to the next. The total number of transitions is limited by the condition that the neglected transitions contribute $< 1\%$ of the total flux, as estimated from the trial solution. Transitions are treated self-consistently when the density of scattered photons at the cloud center, again estimated from the trial solution, exceeds 0.1% of its equilibrium value. The calculated intensities of the observable millimeter wavelength lines are unaffected by the treatment of the highest energy levels.

The two-level results for spherical geometry, which

appear in part (b) of this section, were derived by formal solution of the radiative transfer equation, using the source functions given by Kunasz and Hummer (1974a).

ii) Sobolev Approximation

In the Sobolev approximation, the radiative transfer problem remains nonlinear; but it may be solved locally, so that the scale of the numerical problem is reduced dramatically. Our mathematical formulation of the problem follows that of Lucy (1971); but it is equivalent to that clearly presented for the molecular line problem by de Jong, Chu, and Dalgarno (1975), and need not be repeated here. The calculations assume complete redistribution and adopt the Eddington approximation. The number of transitions included in the multilevel calculations is varied according to the same conditions applied in the microturbulent approximation.

iii) Comparison of Results

To ensure comparable line widths in the two approximations, a uniform velocity gradient was assumed in the Sobolev calculations, with the velocity difference (V) between the center and edge of the cloud set equal to the microturbulent Doppler parameter

$$v_D = \left(\frac{2kT}{m} + v_t^2 \right)^{1/2}.$$

For the comparisons of plane-parallel with spherical geometry, the slab thickness and sphere diameter ($2R$) were taken to be equal.

Numerical results are presented only for the specific intensities emitted perpendicular to the cloud surface, which correspond to observations toward the center of an extended source. Intensity variations across a source depend sensitively on variations in physical conditions through the cloud, and especially on the cloud shape. The simple cloud model considered in this section is too crude for interpretation of source maps, even if plane-parallel cloud models could realistically serve such a purpose.

b) The Two-Level Molecule

In general, the intensity of a spectral line emitted by a diffuse gas depends on the temperature and density of the gas, the abundance of the radiating molecule, the profile of the line, the shape of the cloud, and the details of the molecular structure and transition probabilities. For a two-level molecule, the complications due to molecular structure are suppressed, and the effects of the physical conditions on line strength can be economically presented. The effect of the velocity field on line shape and the effect of cloud geometry can then be isolated and compared.

We first consider the peak intensity of the spectral line. In the Sobolev approximation, the specific intensity I_ν at any frequency ν in the line is given by

$$I_\nu - I_b = [S - I_b][1 - \exp(-\tau_\nu)], \quad (1)$$

where I_b is the intensity of the background radiation (assumed isotropic), S is the line source function, and τ_ν is the optical depth of the line along the chosen line of sight. For the direction normal to the surface of the cloud,

$$\tau_\nu = \kappa(r) / \left(v_D^{-1} \frac{dv}{dr} \right), \quad (2)$$

where the assumed velocity law uniquely relates a position r in the cloud to a frequency ν in the line. In the usual notation,

$$\kappa = \frac{8\pi^3 \mu_{12}^2}{3hv_D} (n_1/g_1 - n_2/g_2), \quad (3)$$

and $v_D = v_{th} = (2kT/m)^{1/2}$. For the assumed linear collapse,

$$v_D^{-1} \frac{dv}{dr} = V/v_D R \quad (4)$$

everywhere in the cloud, and for homogeneous physical conditions κ and S are constant, so that

$$\tau_\nu = \kappa R / (V/v_D), \quad \text{Sobolev}, \quad (5)$$

at each frequency in the line, and I_ν is independent of ν .

In the microturbulent approximation, S generally varies with position in the cloud, and $I_\nu - I_b$ is given by the usual integral form of the equation of transfer. It will suffice here to consider two special cases. If the cloud is optically thin, equation (1) applies, with the peak intensity corresponding to the line center optical depth:

$$\tau_0 = \pi^{-1/2} \int_0^{2R} \kappa dr, \quad \text{microturbulent}. \quad (6)$$

If the cloud is optically thick, the Eddington-Barbier relation associates I_ν with the source function at monochromatic optical depth unity. This accounts for the characteristically self-reversed line profiles, because the line center intensity corresponds to S near the cloud surface, while the maximum intensity, I_m , occurs away from the line center at a frequency such that $\tau_\nu \approx 1$, and reflects the larger source function deep in the cloud. If the maximum value of the source function is S_m , then

$$I_m - I_b \approx S_m - I_b. \quad (7)$$

We emphasize that S_m is the source function at the cloud center, and that *the commonly encountered statement that the observer cannot see deep into the cloud in the microturbulent case is generally incorrect.*

To proceed further, we utilize the particularly simple expression for the source function that follows from the two-level statistical equilibrium equation. Using the photon escape probability β to eliminate the mean intensity of line radiation (Goldreich and Kwan 1974; de Jong, Chu, and Dalgarno 1975), the

expression for the source function at a given point in the cloud becomes

$$S = \frac{\beta}{\beta + \epsilon} I_b + \frac{\epsilon}{\beta + \epsilon} b_\nu(T), \quad (8)$$

where b_ν is the Planck function at the local kinetic temperature, T ,

$$\epsilon = C_{21}/A_{21}[1 - \exp(-h\nu/kT)], \quad (9)$$

C_{21} is the downward collision rate, and A_{21} is the Einstein coefficient for spontaneous emission. In the Sobolev approximation, β is determined locally and can be expressed

$$\beta = [1 - \exp(-a\tau_0)]/a\tau_0, \quad (10)$$

where τ_0 is given by equation (5), and the geometrical factor a is 1 for the spherical case and 3 for the Eddington approximate plane-parallel case. In the microturbulent approximation, β varies with position in the cloud. However, for the optically thin case $\beta \approx 1$, and in the optically thick case, β can be approximated by the probability, P_e , that a photon is emitted sufficiently far in the line wings that the cloud is transparent. For escape from the center of a plane-parallel cloud with a Doppler absorption profile,

$$P_e \approx [\tau_0(\pi \ln \tau_0/2)^{1/2}]^{-1}, \quad (11)$$

where τ_0 is given by equation (6) (Athay 1972, pp. 22 ff.); for a spherical cloud, P_e is larger by a factor Q , where $1 \leq Q \leq 2$ (Kunasz and Hummer 1974a). Thus, except for the logarithmic factor, β has the same dependence on optical depth in both the Sobolev and the microturbulent approximations, a fact that was noted by de Jong, Chu, and Dalgarno (1975).³

Use of the above expressions for the escape probabilities and substitution for S from equation (8) yields, in the optically thin case,

$$I_m - I_b = \frac{\epsilon\tau_0}{1 + \epsilon} (b_\nu(T) - I_b). \quad (12)$$

In the optically thick case, $\beta \approx (c\tau_0)^{-1}$, where c includes the influence of both the geometry and the velocity field, so

$$I_m - I_b = \frac{c\epsilon\tau_0}{1 + c\epsilon\tau_0} (b_\nu(T) - I_b). \quad (13)$$

Equations (12) and (13) express the dependence of the peak intensity on physical conditions, transition

³ In a sense, this agreement is fortuitous, because β is independent of the assumed absorption profile in the Sobolev approximation, but depends on the shape of the line wings in the microturbulent case. However, for an exponential line profile, which may result from supersonic turbulence (Münch 1957; Hobbs 1969), $P_e \approx 1/\tau_0$ in the plane-parallel case, so that the agreement is preserved. Line profiles having still more extensive (e.g., damping) wings, which could give more significant changes in β , seem unlikely to occur for the observed molecular lines.

probabilities, velocity field, and geometry. The temperature establishes the scale of intensities, so the relations can be compactly represented if $I_m - I_b$ is normalized to its equilibrium value. The cloud density, the molecular abundance, and the transition probabilities determine the fractional thermalization through the product $\epsilon\tau_0$, as discussed for the spherical Sobolev case by Goldreich and Kwan (1974). Instead of $\epsilon\tau_0$, we use the factor $\lambda\tau_0$, with $\lambda = \epsilon/(1 + \epsilon)$, as the abscissa in Figure 1a, because this choice combines the results for the optically thin and optically thick regimes, and substantially isolates the effects of the velocity field and cloud geometry on the peak intensities.

Figure 1a presents numerical results for the normalized peak intensity emitted by two-level molecules in isothermal homogeneous clouds. The curves in the figure display the basic similarity expected from the common variation of the photon escape probability with optical depth in the cases considered. They also show the differences associated with the velocity-geometry factor c in equation (13), amplified in the microturbulent cases by the effect of self-absorption on the line profiles. The intensity differences attributable to the choice of velocity field are comparable to those due to the shape of the cloud (about a factor of 3). Hence, the Sobolev and microturbulent approximations yield peak intensities which agree within the relatively fundamental uncertainty imposed by ignorance of molecular cloud geometries. It is noteworthy that the Sobolev slab case, in which photons suffer an unrealistic geometrical limitation to escape from the cloud, differs most from the other cases.

The integrated intensities of the lines exhibit even closer agreement than the peak intensities, for reasons which depend, not on the circumstantial agreement between the escape probabilities, but on the characteristics of line emission from *effectively thin* media. Effectively thin clouds resemble optically thin clouds in local thermodynamic equilibrium (LTE): virtually every photon created by collisional excitation and radiative de-excitation of a molecule, though it may scatter many times, ultimately escapes the cloud. Hence, *independent of the velocity field*, the flux integrated over frequency (H) is simply proportional to the rate of collisional excitation and to the projected density of molecules. Quite generally, for $\beta \gg \epsilon$, one finds

$$H = \frac{v}{c} \int_0^{2R} \epsilon [b_\nu(T) - I_b] v_D \kappa dr, \quad \text{slab}, \quad (14a)$$

$$H = \frac{v}{c} \int_0^R \epsilon [b_\nu(T) - I_b] v_D \kappa \left(\frac{r}{R}\right)^2 dr, \quad \text{sphere}, \quad (14b)$$

while once again, in the optically thin case, one can replace ϵ with λ . Restricting attention to the special cases considered in this section, one may write for both geometries:

$$H = g \frac{v}{c} \Delta v_{1/2} (b_\nu(T) - I_b) \epsilon \tau_0, \quad (15)$$

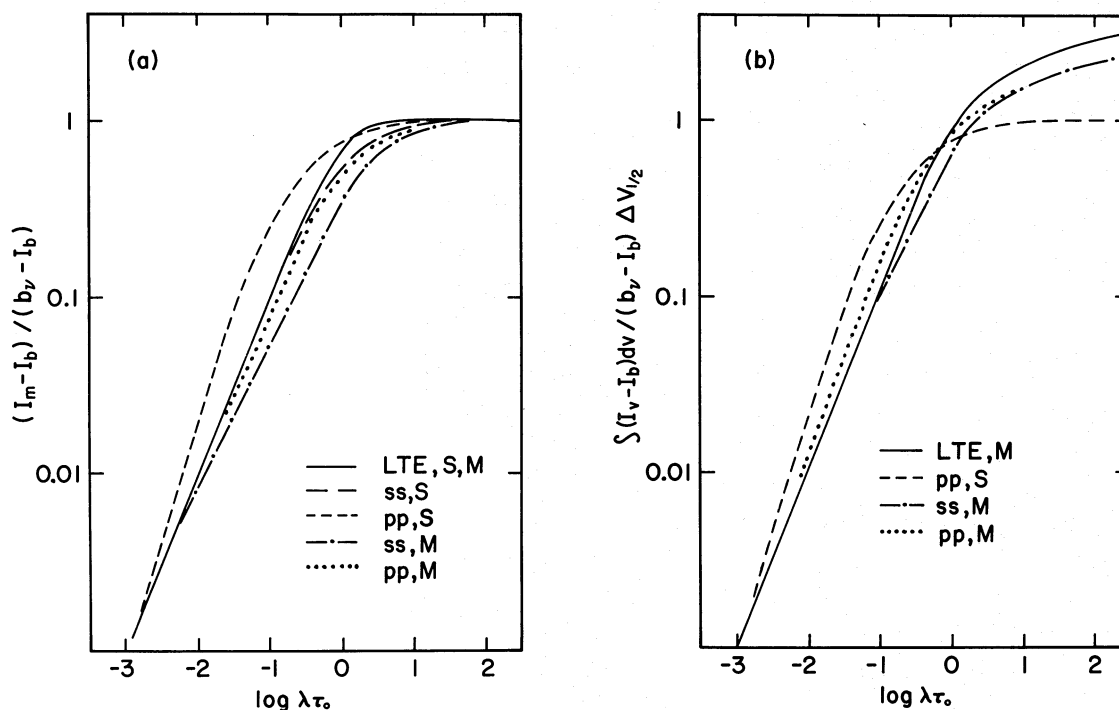


FIG. 1.—(a) Comparison of peak line intensities emitted normal to the cloud surface by a two-level molecule in an isothermal homogeneous cloud, for slab (pp) and spherical (ss) geometries in the Sobolev (S) and microturbulent (M) approximations, for $\lambda = 1$ (solid line, LTE) and $\lambda = 10^{-2}$. The LTE relationship [eq. (1) with $S = b_\nu(T)$] is the same for all four cases. Note that for $\lambda = 10^{-2}$, the curves depart from the solid line when $\tau_0 \sim 1$. (b) Normally emergent intensities integrated over velocity, normalized as suggested by eq. (15), for the microturbulent approximation and the same conditions as in (a). The plane-parallel Sobolev and LTE Sobolev curves, which are omitted for the sake of clarity, are identical to the corresponding curves in (a).

where $\Delta v_{1/2}$ is the full width at half-maximum (FWHM) of optically thin lines, i.e., $2V$ in the Sobolev approximation, and $2(\ln 2)^{1/2} v_D$ in the microturbulent approximation, and g is a geometrical factor which approximately equalizes the volume emissivities of the clouds ($g \approx 1$ for the slab and $g \approx 1/6$ for the sphere in the microturbulent case, with strict equality in the Sobolev case). Equation (15) describes the linear portion of the non-LTE curve of growth, which extends to $\tau_0 \sim \epsilon^{-1}$ for the Sobolev and microturbulent cases.⁴

Figure 1b illustrates the dependence on physical conditions exhibited by the normally emergent integrated intensity. Not surprisingly, the figure shows that, for nonthermalized lines, the integrated intensities vary in proportion to the total flux, as expressed by equation (15). They are more sensitive to the cloud shape than to the velocity distribution, even though the geometrical effects are minimized by observation perpendicular to the cloud surface. For thermalized lines, the integrated intensities depend strongly on the velocity distribution, because the lines fall on the Doppler part of the curve of growth.

For the very simple cloud model considered here, both the Sobolev and microturbulent approximations

⁴ For a stationary cloud with a Lorentz line profile, $\beta \approx \tau_0^{-1/2}$, and the linear part of the curve of growth extends to $\tau_0 \approx \epsilon^{-2}$ (Athay 1972, pp. 22, 29, 192–193).

yield unrealistic line profiles, and further comparison is unwarranted. For a macroturbulent cloud, it is clear that the integrated intensities must follow the relationships illustrated in Figure 1b. In this case one cannot write down simple expressions for β or τ_ν . But as long as the line width is insensitive to optical depth, variations in the integrated intensity emitted by effectively thin clouds must be matched by variation in the peak intensity, yielding curves similar to those in Figure 1a.

c) Carbon Monoxide

The relative insensitivity of peak and integrated line intensities to velocity fields, demonstrated in part (b) of this section for a two-level molecule, persists when a realistic molecular model is introduced. To show this, we present calculations made for carbon monoxide, using the Green and Thaddeus (1976) cross sections for collisional excitation by H_2 , fitted to the empirical form adopted by de Jong, Chu, and Dalgarno (1975).⁵

⁵ After several trials involving fits over different temperature ranges, a single least-squares fit to the collision rates at all temperatures treated by Green and Thaddeus was adopted for each value of ΔJ . The derived constants differ somewhat from those of de Jong, Chu, and Dalgarno, but represent the rates within their theoretical uncertainties (Green, private communication).

The multilevel results do not admit the compact representation that is possible for the two-level case. The parameter λ cannot be satisfactorily defined, because collisions are not restricted to follow the radiative selection rules, and τ_0 depends on the excitation of all the energy levels. Hence it is preferable to abandon the two-level parameters, and to use contour diagrams to display the calculated intensities for the $J = 1 \rightarrow 0$ or the $J = 2 \rightarrow 1$ line or the intensity ratio between the two lines. For a specified cloud temperature, the adopted independent variables are the molecular hydrogen density, $n_{\text{H}_2}(\text{cm}^{-3})$, and the projected density of CO molecules per unit velocity between the surface and the center of the cloud, N_{CO}/v ($\text{cm}^{-2}/\text{km s}^{-1}$), where

$$N_{\text{CO}}/v = n_{\text{CO}}/(dv/dr) = n_{\text{CO}}R/V, \quad \text{Sobolev,} \quad (16a)$$

$$N_{\text{CO}}/v = \int_0^R n_{\text{CO}} dr/v_D = n_{\text{CO}}R/v_D, \quad \text{microturbulent.} \quad (16b)$$

To facilitate comparison with observation, the intensities are expressed in terms of the peak line temperature emitted normal to the cloud surface,

$$T_m = \frac{c^2}{2kv^2} (I_m - I_b), \quad (17)$$

where $I_b = b_\nu(2.7 \text{ K})$, or in terms of the corresponding integrated line temperature, normalized as in Figure 1*b* to the optically thin line width, i.e., $\int T_l dv/\Delta v_{1/2}$.

In each panel of Figures 2–6, the solid contours show the results of the microturbulent slab calculations, with representative contours for the Sobolev slab and sphere given for comparison. We have not calculated contours for the microturbulent sphere; but the consistency of the velocity-geometry effects between the CO results and the two-level calculations provides assurance that this omission will not invalidate our discussion. The contour shapes in each of the diagrams are insensitive to velocity field and cloud geometry. Moreover, comparison of parts (a) and (b) of Figures 2, 3, and 4 reveals that, as in the two-level case, the appearance of the contours is very similar for both the peak intensities and the integrated intensities. Thus, with one exception, these three figures are discussed without specific reference to parts (a) or (b), and only integrated line temperature contours are subsequently presented in Figures 5 and 6.

Figures 2 and 3 illustrate the dependence of line temperature on density and molecular abundance at constant temperature, $T = 30 \text{ K}$. For both the $J = 1 \rightarrow 0$ line (Figure 2) and the $J = 2 \rightarrow 1$ line (Fig. 3), the contours become independent of density at large n_{H_2} , where collisions thermalize the excitation. At low densities the contours are diagonal, reflecting the dependence of the emitted line intensities on the product $n_{\text{H}_2}N_{\text{CO}}/v$ (cf. eqs. [13] and [15]). Between these limits, at $n_{\text{H}_2} \sim 10^3 \text{ cm}^{-3}$, the line temperatures exceed their LTE values by factors as large as 2.2 for $J = 1 \rightarrow 0$, and 1.2 for $J = 2 \rightarrow 1$, producing

bulges in the contours toward smaller N_{CO}/v . This intensity enhancement results from the predominance of multipole collisional excitations and the tendency of such excitations, when followed by spontaneous emission, to overpopulate the upper levels of the transitions (especially $J = 1$; Goldsmith 1972). Since it is primarily due to collisional excitation, the enhancement is largest for optically thin lines, and diminishes as the lines approach thermalization.

Figure 4 indicates more clearly than Figures 2 and 3 how observation of the two transitions can determine the physical conditions in molecular clouds. Like the individual line temperature contours, the ratio contours become vertical at large n_{H_2} and diagonal at small n_{H_2} , which indicates that both transitions yield essentially the same information under these conditions. At intermediate densities and large N_{CO}/v , both lines become thermalized, so the intensity ratio is a poor diagnostic of density or molecular abundance; but it does serve to validate the use of either line as a temperature indicator. For effectively thin lines at these densities, the ratio contours run transverse to the line temperature contours, so that, in principle, observations of the two lines quite accurately determine both the density and the molecular abundance. Moreover, the availability of isotopic species with widely different abundances ensures that this approach can be readily utilized.

The separations between the line temperature contours representing the different velocity-geometry cases in Figures 2 and 3 correspond quite accurately to the intensity differences found in the two-level cases (cf. Fig. 1, which is analogous to a plot of line temperature against N_{CO}/v at constant n_{H_2}). The differences, of course, are small at high densities. At low densities for effectively thin lines, the differences increase to factors ~ 3 , the most intense lines arising in the Sobolev slab case, with its smaller escape probabilities. The differences approach an order of magnitude for lines which are nearly thermalized, corresponding to the knee of the curves in Figure 1. Here the effects of the velocity field and cloud shape are paramount, and the observer is ill-advised to draw conclusions from small intensity differences.

An important implication of these model-dependent effects concerns the derivation of isotope ratios from molecular line intensities. For example, all four velocity-geometry cases predict the same intensities for optically thin lines (cf. Fig. 1), but threefold differences emerge in the optically thick regime. Hence, the derivation of an isotope ratio from two nonthermalized lines when one is optically thick and one is optically thin can lead to results which differ by factors ~ 3 between different velocity-geometry models.

The ratio contours (Fig. 4) show slightly more sensitivity to velocity and geometry than the line temperature contours themselves. The most conspicuous deviation between solid and dashed curves occurs for the contours representing line temperature ratios equal to 1. The low escape probability in the Sobolev slab case causes the $J = 2 \rightarrow 1$ line to reach

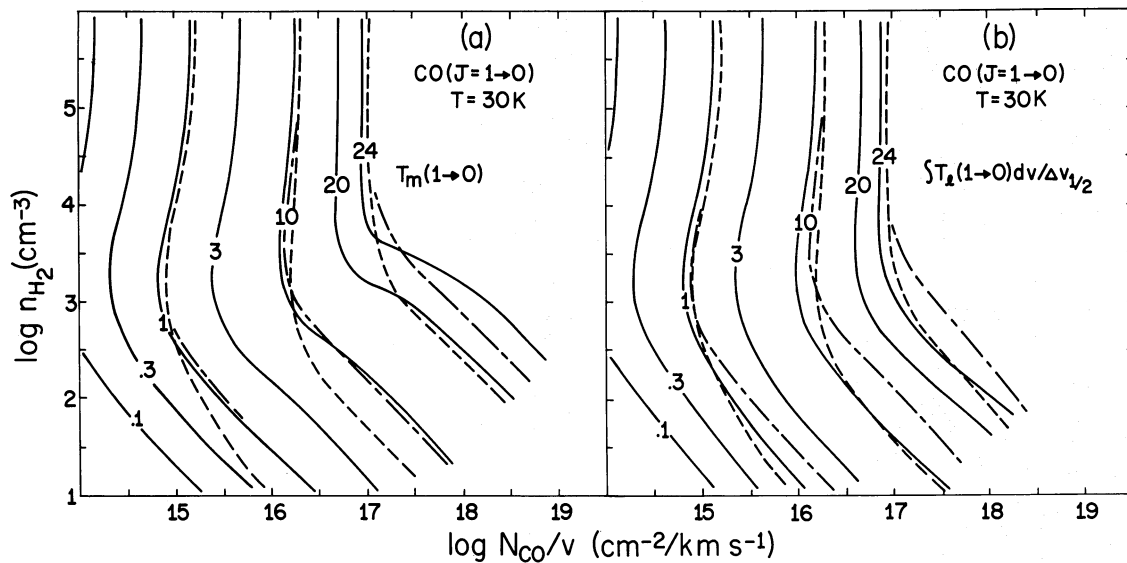


FIG. 2.—(a) Comparison of the peak line temperatures emitted by homogeneous clouds at 30 K in the CO $J = 1 \rightarrow 0$ transition. The contours of $T_m(1 \rightarrow 0)$ in kelvins are presented as functions of n_{H_2} and N_{CO}/v for the microturbulent slab (solid line), the Sobolev slab (dashed line), and Sobolev sphere (dash-dot line) cases. (b) Comparison of the integrated line temperature contours for the CO $J = 1 \rightarrow 0$ transition.

a given intensity at systematically lower densities than in the other cases. However, even here the differences in physical conditions deduced for given line temperatures hardly exceed a factor of 3, except for large N_{CO}/v in Figure 4b. In that case, the wide divergence between the microturbulent and Sobolev contours simply reflects the divergence in the “flat” portions of the curves of growth, as shown in Figure 1b.

Figures 5 and 6 present the contour diagrams for $T = 5$ K and 100 K, respectively. They show that both the general dependence of line temperature on physical conditions and the effects of velocity field

and cloud geometry are insensitive to kinetic temperature. However, two temperature-sensitive effects warrant further comment.

1. The “bulge” in the line temperature contours due to the multipole collisions grows as the temperature increases. It is absent at 5 K, while at 100 K, the excess over LTE reaches a factor 5.9 for $J = 1 \rightarrow 0$ and 2.6 for $J = 2 \rightarrow 1$. At 100 K, a population inversion occurs in the $J = 1 \rightarrow 0$ transition for $n_{\text{H}_2} \sim 10^4 \text{ cm}^{-3}$ and low N_{CO}/v , but it produces no noticeable effects in the emergent intensities. In fact, the maximum intensity enhancement occurs at slightly

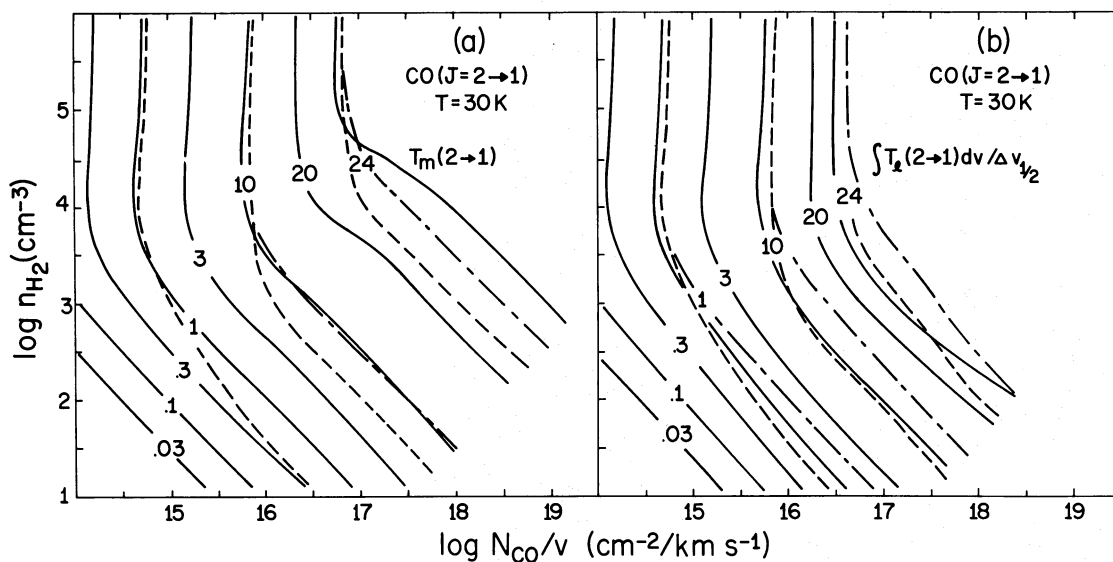


FIG. 3.—Same as Fig. 2, for the CO $J = 2 \rightarrow 1$ transition

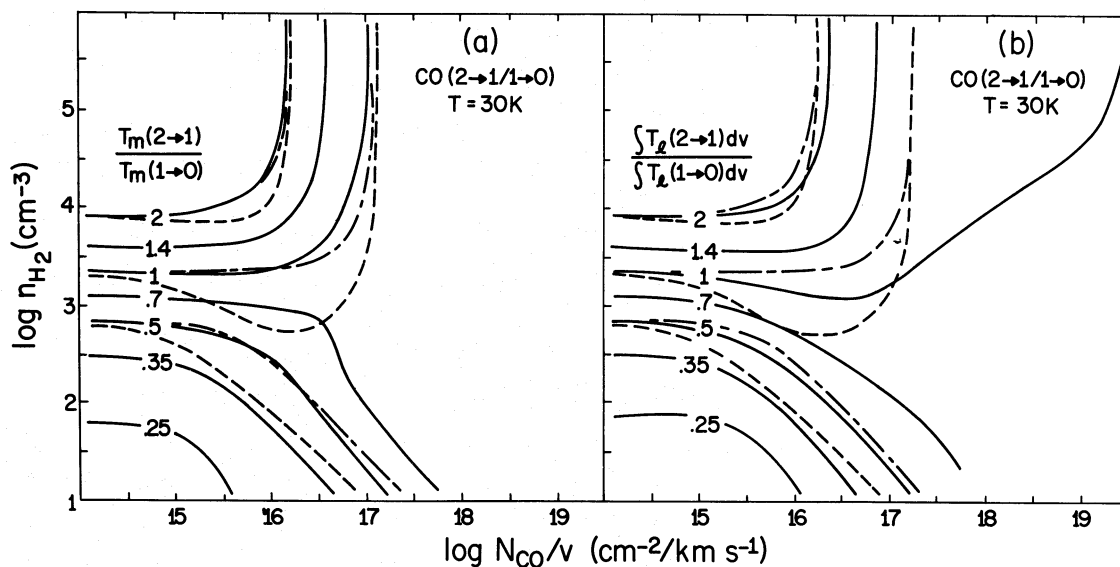


FIG. 4.—Comparison of the ratios of the peak line temperatures (a) and integrated line temperatures (b), for the same conditions as in Figs. 2 and 3.

lower densities, and, in any event, the effectiveness of the collisional pumping declines as the line radiation fields build up. Leung and Liszt (1976) have remarked upon the intensity enhancement and derived CO abundances appreciably smaller than previous estimates. Since their discussion is based on $^{12}\text{CO}/^{13}\text{CO}$ intensity ratios, however, it rests not only on the enhanced ^{13}CO intensities, which are insensitive to velocity and geometry, but also on the slow approach of the ^{12}CO lines to thermalization. The latter feature is very model-sensitive, and we expect it to be very slow for their microturbulent sphere models (cf. Fig. 1). Hence, the low CO/H_2 abundance ratio which they derive must be viewed with caution.

2. At $T = 100$ K and low densities, the $J = 1 \rightarrow 0$ and $J = 2 \rightarrow 1$ line temperatures (Figs. 6a, 6b) approach equality for $\int T_i dv / \Delta v_{1/2} \sim 10$ K, and grow only very slowly with further increases in N_{CO}/v . This slow intensity variation reflects decreases in the relative populations of the lowest energy levels, which partially compensate for increases in column density. This effect must occur whenever cloud temperatures are sufficiently high that many energy levels become significantly populated. Under such conditions neither line serves as a reliable indicator of density or CO abundance; small intensity differences between models lead to wide differences in the location of the contour representing equal line strengths (Fig. 6c). Moreover, in this case, as opposed to the situation at $T = 30$ K, near-equality between the $J = 1 \rightarrow 0$ and $J = 2 \rightarrow 1$ line temperatures does not necessarily justify their use as temperature indicators. However, these effects are predicted only for clouds which have the improbable combination of high temperature with high N_{CO}/v and low n_{H_2} .

IV. DISCUSSION

This paper proceeds from the premise that the dynamics of molecular clouds is too complex to be precisely described either in terms of microturbulence or in terms of simple systematic motions, and its purpose is to evaluate the implied uncertainties in the interpretation of molecular cloud spectra. It advances the view that these two simple assumptions about the velocity field represent alternative approximations in which scattered radiation does or does not mediate interactions among molecules in diverse parts of the cloud. Then, by comparison of the intensities calculated in the two approximations for isothermal homogeneous clouds, the paper provides an initial estimate of the velocity-dependent uncertainties in molecular line analysis.

The calculations presented lead to the following conclusions.

1. For effectively thin (nonthermalized) molecular emission lines—which usually include all but the lines of ^{12}CO —analyzed using isothermal homogeneous cloud models, the simplifying assumptions made concerning the velocity field and cloud geometry produce comparable uncertainties (factors ~ 3) in the derived values of density and molecular abundance. Lines which are near thermalization, like those of ^{13}CO , yield good estimates of the cloud temperature, but give values of density and molecular abundance that are extremely model-sensitive.

2. Within the uncertainties introduced by ignorance of cloud shape, the various studies which use the simple cloud model adopted in this paper may confidently utilize the relatively simple mathematical apparatus of the Sobolev approximation, without

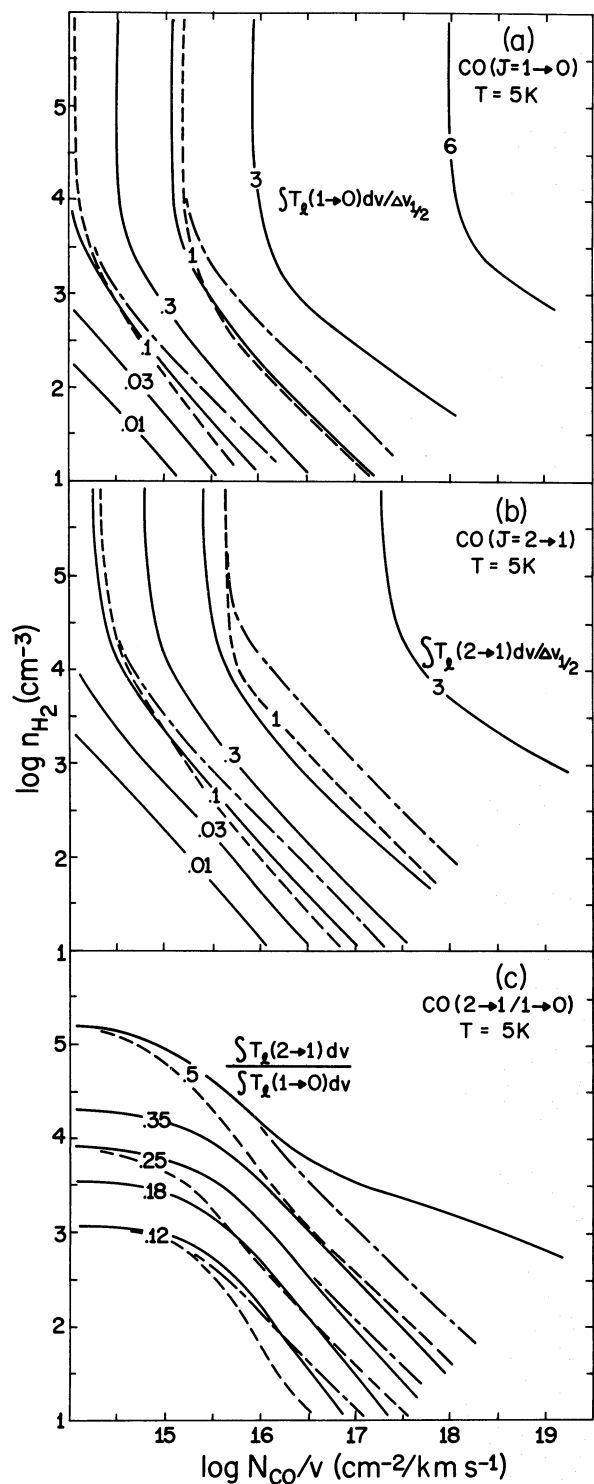


FIG. 5.—Comparison of integrated line temperatures, as in parts (b) of Figs. 2, 3, and 4, for $T = 5$ K.

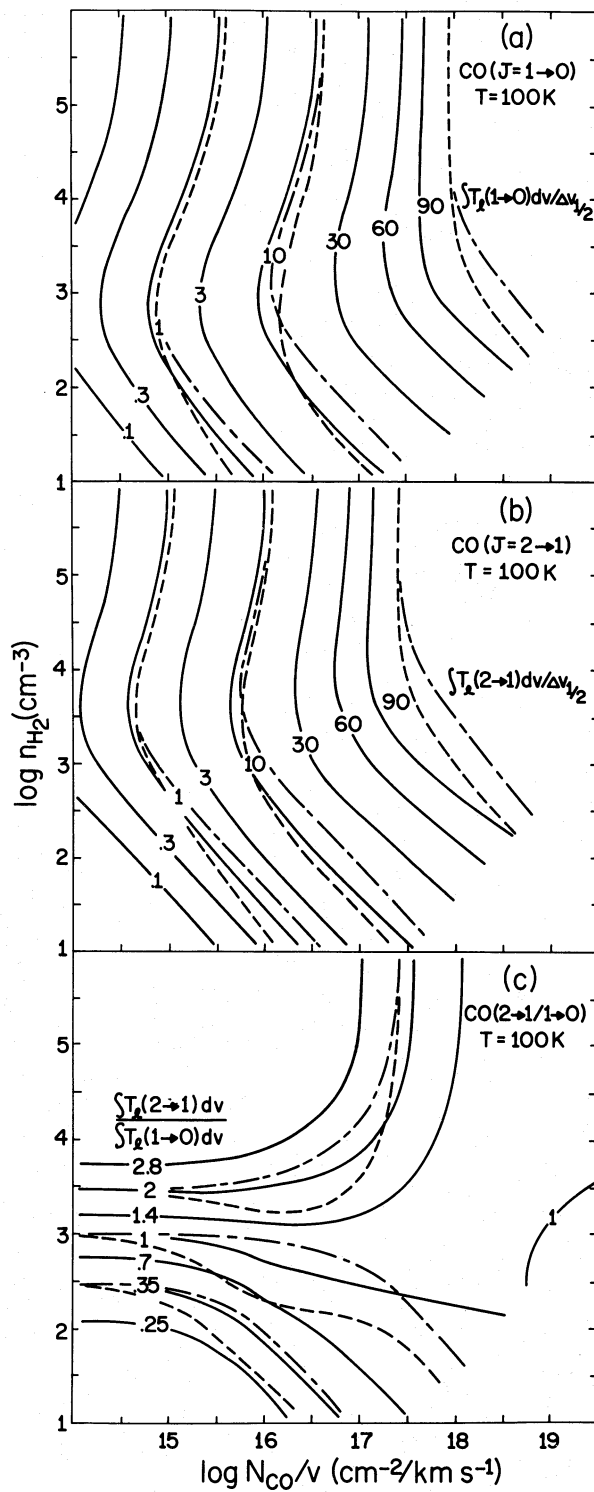


FIG. 6.—Same as Fig. 5, for $T = 100$ K

regard to the true line-broadening mechanism. For such work it is better to use spherical cloud models, both because plane-parallel geometry is physically unrealistic, and because for given physical conditions the Sobolev slab case yields line temperatures at one extreme of the range found in this paper.

To the extent that the microturbulent and Sobolev approximations yield similar results, comparison between the two cases provides no information about the dynamics of molecular clouds. For more realistic inhomogeneous cloud models, the two approximations will most likely predict larger intensity differences, especially because the effects of nonlocal radiative excitation will be more apparent in the microturbulent results. However, it seems probable that such comparisons will merely delimit the range of cloud parameters which yield intensity distributions in agreement with observed source maps, rather than dictate a choice between the velocity models. Line profile analysis can provide a more exacting test of the models, but the microturbulent approximation

is too simplistic to pass such a test. However, microturbulent source functions might be used with approximate "macro-turbulent" velocity distributions to generate more realistic line shapes. Such a procedure is not self-consistent, but it could help to clarify what kinds of motion dominate line formation in molecular clouds.

The calculations reported in this paper utilized the IBM 360/95 computer at the Goddard Institute for Space Studies. The author expresses his thanks to Dr. Robert Jastrow, Director of the Institute, and especially to Dr. Patrick Thaddeus, for support during the course of this work. The author further acknowledges support from NSF grant MPS 73-04949 to the Five College Radio Astronomy Observatory. The Five College Radio Astronomy Observatory is operated with the cooperation of the Metropolitan District Commission of the Commonwealth of Massachusetts.

REFERENCES

- Arons, J., and Max, C. E. 1975, *Ap. J. (Letters)*, **196**, L77.
 Athay, R. G. 1972, *Radiative Transport in Spectral Lines* (Dordrecht: Reidel).
 Auer, L. H. 1971, *J. Quant. Spectrosc. Rad. Transf.*, **11**, 573.
 ———. 1973, *Ap. J.*, **180**, 469.
 Avrett, E. H., and Hummer, D. G. 1965, *M.N.R.A.S.*, **130**, 295.
 Clark, F. O., Buhl, D., and Snyder, L. E. 1974, *Ap. J.*, **190**, 545.
 de Jong, T., Chu, S.-I., and Dalgarno, A. 1975, *Ap. J.*, **199**, 69.
 Feautrier, P. 1964, *C.R. Acad. Sci. Paris*, **258**, 3189.
 Goldreich, P., and Kwan, J. 1974, *Ap. J.*, **189**, 441.
 Goldsmith, P. F. 1972, *Ap. J.*, **176**, 597.
 Green, S., and Thaddeus, P. 1976, *Ap. J.*, **205**, 766.
 Hobbs, L. M. 1969, *Ap. J.*, **157**, 165.
 Hummer, D. G. 1969, *M.N.R.A.S.*, **145**, 95.
 Kunasz, P. B., and Hummer, D. G. 1974a, *M.N.R.A.S.*, **166**, 19.
 ———. 1974b, *M.N.R.A.S.*, **166**, 57.
 Kutner, M. L., and Tucker, K. D. 1975, *Ap. J.*, **199**, 79.
 Leung, C. M. 1975, *Ap. J.*, **199**, 340.
 Leung, C. M., and Liszt, H. S. 1976, *Ap. J.*, **208**, 732.
 Liszt, H. S., Wilson, R. W., Penzias, A. A., Jefferts, K. B., Wannier, P. G., and Solomon, P. M. 1974, *Ap. J.*, **190**, 557.
 Lucas, R. 1974, *Astr. Ap.*, **36**, 465.
 Lucy, L. B. 1971, *Ap. J.*, **163**, 95.
 Mihalas, D. 1970, *Stellar Atmospheres* (San Francisco: Freeman).
 Morris, M., Zuckerman, B., Turner, B. E., and Palmer, P. 1974, *Ap. J. (Letters)*, **192**, L27.
 Münch, G. 1957, *Ap. J.*, **125**, 42.
 Rybicki, G. B. 1971, *J. Quant. Spectrosc. Rad. Transf.*, **11**, 589.
 Scoville, N. Z., and Solomon, P. M. 1974, *Ap. J. (Letters)*, **187**, L67.
 Sobolev, V. V. 1960, *Moving Envelopes of Stars* (Cambridge: Harvard University Press).
 White, R. E. 1971, Ph.D. thesis, Columbia University.
 ———. 1973, *Bull. AAS*, **5**, 421.
 Zuckerman, B., and Evans, N. J., II. 1974, *Ap. J. (Letters)*, **192**, L149.

RICHARD E. WHITE: Five College Astronomy Department, Clark Science Center, Smith College, Northampton, MA 01060